A metabolic pathway leading to mannosylfructose biosynthesis in *Agrobacterium tumefaciens* uncovers a family of mannosyltransferases

Leticia L. Torres and Graciela L. Salerno*

Centro de Investigaciones Biológicas, Fundación para Investigaciones Biológicas Aplicadas, Casilla de Correo, 1348, 7600 Mar del Plata, Argentina

Communicated by Bob B. Buchanan, University of California, Berkeley, CA, July 17, 2007 (received for review October 4, 2006)

A metabolic pathway for biosynthesis of the nonreducing disaccharide mannosylfructose (β-fructofuranosyl-α-mannopyranoside), an important osmolyte in *Agrobacterium tumefaciens*, was discovered. We have identified and functionally characterized two ORFs that correspond to genes (named *mfpsA* and *mfppA*) encoding the rare enzymes mannosylfructose-phosphate synthase and mannosylfructose-phosphate phosphatase, an associated phosphohydrolase. The *mfpsA* and *mfppA* genes are arranged in an operon structure, whose transcription is up-regulated by NaCl, resulting in the accumulation of mannosylfructose in the cells. Not only is the biosynthesis of mannosylfructose mechanistically similar to that of sucrose, but the corresponding genes for the biosynthesis of both disaccharides are also phylogenetic close relatives. Importantly, a protein phylogeny analysis indicated that mannosylfructose-phosphate synthase defines a unique group of mannosyltransferases.

glycosyltransferase evolution | functional diversification | salt stress response | *Agrobacterium*–plant interaction | sucrose

Glycosyl-transfer reactions are of remarkable biological importance on earth because they account for the biosynthesis and hydrolysis of the bulk of biomass (1). According to their sequence similarity and the wide spectrum of sugar donors, glycosyltransferases (GTs) have been organized in 90 families (www.cazy.org/fam/acc_GT.html). Particularly, GTs are involved in the biosynthesis and cleavage of sucrose (Suc), one of the most important nonreducing sugars found in nature, limited to oxygenic photosynthetic organisms. Suc occupies a central role in plant life and is also associated with environmental stress responses in both plants and cyanobacteria (2). The principal Suc-biosynthesis route involves the sequential action of sucrose-phosphate synthase (SPS) (UDP-glucose: D-fructose-6-phosphate 2-α-D-glucosyltransferase, EC 2.4.1.14) and sucrose-phosphate phosphatase (SPP) (sucrose-6^F-phosphate-phosphohydrolase, EC 3.1.3.24) yielding free Suc and P_i (Fig. 1). The hydrolysis of the intermediate sucrose-6P (Suc-6P) by SPP leads to an essentially irreversible pathway, providing an efficient production of Suc even at low substrate concentrations (2, 3).

SPSs and SPPs of extant organisms were proposed to be proteins with multiple domains with a modular architecture that might have arisen from primordial functional domains shuffled during evolution. The biochemical characterization of *Anabaena* (An) sp. PCC 7120 SPSs (An-SPSs), the smallest proteins displaying SPS activity, uncovered a 400-aa region shared by all SPSs, which defined a functional glucosyltransferase domain (GTD). The GTD contains (*i*) a characteristic motif present in all SPSs [(DE)xGGQxxY(VIL)x(DE)] and (*ii*) a motif that is ubiquitous of the nucleotide recognition domain 1α (NRD1α)-GT family [ExFGxxxExxxxxxPxxA(TS)xGG] (4). SPPs are phosphohydrolases, which are members of the haloacid dehalogenase (HAD) superfamily, characterized by a conserved α-/β-domain (hydrolase fold) (5). Note that the characterization of An-SPP, the minimal unit that catalyzes the final step in the Suc biosynthesis pathway, defined a phosphohydrolase domain (PHD) that shares a conserved motif ($DxDxTx_{27}Tx_{119}Kx_{24}DxxxD$) with other phosphohydrolases (4, 5).

On the basis of sequence analysis, homologs to genes coding for SPS and SPP were reported in the genome of the ubiquitous soil proteobacterium *Agrobacterium tumefaciens* (At) (ORFs corresponding to loci AGR_C_1178 and AGR_C_1175) (2). These ORFs showed a cluster organization, suggesting a functional pathway. However, because the ability to synthesize and accumulate Suc had not been reported in nonphotosynthetic microorganisms, we found it of interest to investigate those sequences. Our molecular and biochemical examinations reveal that the products of the *A. tumefaciens* ORFs are not Suc-related proteins. Instead, they are previously undescribed enzymes, mannosylfructose-phosphate synthase (MFPS) and mannosylfructose-phosphate phosphatase (MFPP), defining the pathway that leads to the biosynthesis of mannosylfructose (MF) (β-fructofuranosyl-α-mannopyranoside) and discovering a family of mannosyltransferases (MTs).

Results

Biochemical and Functional Characterization of Recombinant At-GTD and At-PHD. Using as queries An-SPS-A, An-SPS-B, and An-SPP (4, 5), we identified two adjacent overlapping ORFs of 1,365 bp (*At-GTD*) and 747 bp (*At-PHD*) within the *A. tumefaciens* C58 genome (Fig. 2*A*). The *At-GTD*-deduced protein (M_r = 51.9 kDa) has 30% and 31% identity with An-SPS-A and An-SPS-B, respectively, whereas that of *At-PHD* (M_r = 27.2 kDa) shares ≈27% identity with An-SPP.

At-GTD and *At-PHD* expression products were obtained and purified from *Escherichia coli* for further functional characterization (Fig. 2 *B* and *C*, lanes 1–3). Using immunoblot analysis, we showed that His_6::At-GTD and His_6::At-PHD were immunorevealed with anti-An-SPS and anti-An-SPP antibodies, respectively (Fig. 2 *B* and *C*, lanes 4 and 5). However, the notion of At-GTD being an SPS ortholog did not hold because the production of a fructose-containing disaccharide from An-SPS substrates (Fru-6P and XDP-Glc, where X = U, A, or G) (2) was negligible (Fig. 3*A*). In addition, SPS activity could not be detected in *A.*

Author contributions: L.L.T. and G.L.S. designed research; L.L.T. performed research; G.L.S. contributed new reagents/analytic tools; L.L.T. and G.L.S. analyzed data; and L.L.T. and G.L.S. wrote the paper.

The authors declare no conflict of interest.

Abbreviations: An, *Anabaena*; An-SPP, *Anabaena* sp. PCC 7120 SPP; An-SPS, *Anabaena* sp. PCC 7120 SPS; At, *Agrobacterium tumefaciens*; GT, glycosyltransferase; GTD, glucosyltransferase domain; Man, mannose; MF, mannosylfructose; MF-6P, mannosylfructose-6P; MFPP, mannosylfructose-phosphate phosphatase; MFPS, mannosylfructose-phosphate synthase; MT, mannosyltransferase; PHD, phosphohydrolase domain; SPP, sucrose-phosphate phosphatase; SPS, sucrose-phosphate synthase; Suc, sucrose; Suc-6P, sucrose-6P.

Data deposition: The sequences reported in this paper have been deposited in the GenBank database (accession nos. EF530045 and EF530046).

*To whom correspondence should be addressed at: Vieytes 3103, Casilla de Correo, 1348, 7600 Mar del Plata, Argentina. E-mail: gsalerno@fiba.org.ar.

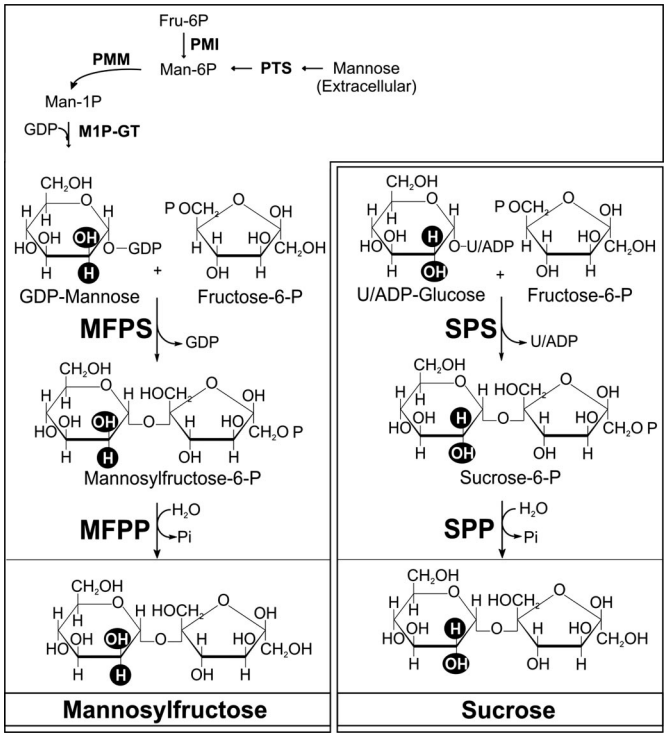

Fig. 1. Biosynthesis pathway of MF. From the *A. tumefaciens* C58 genome annotation, it can be proposed that extracellular mannose can be taken up and phosphorylated by a phosphotransferase system (PTS) (EC 2.7.1.69, Atu0031) yielding Man-6P, which can also be produced from intracellular Fru-6P by Man-6-phosphate isomerase (PMI) (EC 5.3.1.8, Atu3311) activity. The sequential action of phosphomannomutase (PMM) (EC 5.4.2.8, Atu2379) and Man-1P-guanylyl transferase (M-1P-GT) (EC 2.7.7.22, Atu3353) leads to the synthesis of GDP-Man, the mannosyl donor for MF biosynthesis. The Suc biosynthesis pathway in plants and *Anabaena* sp. PCC 7120 (2, 13, 14) is shown for comparison.

tumefaciens cell-free extracts (data not shown). The catalytic activity of His_6::At-GTD was assayed with other glycosyl donors as GDP-mannose (Man), ADP-Man, and UDP-Man. A fructose-

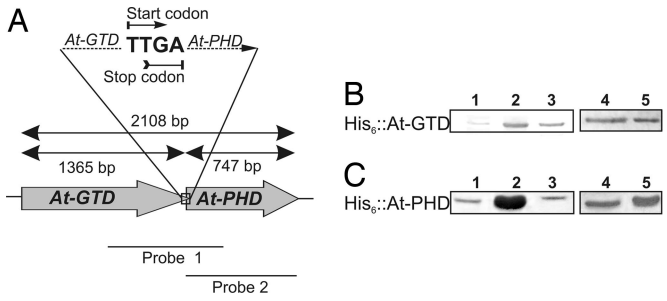

Fig. 2. Genomic organization and heterologous expression of two *A. tumefaciens* C58 ORFs (locus AGR_C_1178 and locus AGR_C_1175, here named *At-GTD* and *At-PHD*, respectively) homologous to Suc biosynthesis genes. (*A*) Schematic representation of the ORF overlapping. (*B* and *C*) Expression in *E. coli* cells of *At-GTD* and *At-PHD*, respectively. *E. coli* polypeptides were separated by SDS/PAGE and stained with Coomassie blue (lanes 1–3). Lanes 1 and 2, protein extracts from noninduced and isopropyl-β-D-thiogalactopyranoside-induced *E. coli* cells, respectively; lane 3, purified His_6-tagged recombinant protein; lanes 4 and 5, immunoblot analysis revealed with polyclonal antibodies against *Anabaena* SPS-A (anti-An-SPS) or SPP (anti-An-SPP) (*B* and *C*, respectively); lane 4, affinity-purified His_6-tagged recombinant proteins; lane 5, purified recombinant An-SPS-A (*B*) or An-SPP (*C*) (4, 6). Figures are representative of three independent experiments.

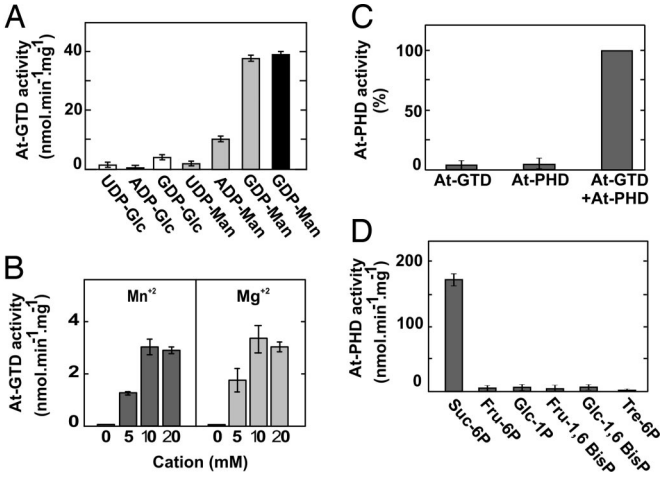

Fig. 3. Biochemical characterization of recombinant At-GTD and At-PHD. (*A*) His_6::At-GTD substrate specificity. Aliquots of purified His_6::At-GTD were assayed in reaction mixtures containing 10 mM XDP-Glc (open bars) or 3 mM XDP-Man (gray bars). Enzyme activity was measured as the production of fructose-containing disaccharides (open and gray bars) or by quantifying GDP (black bar). (*B*) Effect of divalent cations on His_6::At-GTD activity. (*C*) Phosphatase activity assayed on the product of the reaction catalyzed by His_6::At-GTD. The reaction mixture contained 3 mM GDP-Man, 10 mM Fru-6P, 10 mM $MgCl_2$, 100 mM Hepes-NaOH (pH 7.0), and aliquots of the indicated recombinant proteins. P_i formation was determined after a 30-min incubation. (*D*) His_6::At-PHD substrate specificity. Sugar phosphates were assayed at 1 mM final concentration. Values are the mean ± SD; $n = 3$.

containing sugar was produced mainly with GDP-Man as substrate and, in a minor extent, in the presence of ADP-Man (Fig. 3*A*). The reaction products (assayed with GDP-Man) were identified as a phosphorylated nonreducing disaccharide composed of one mannose and one fructose residue (named mannosylfructose-6P, MF-6P) and GDP (data not shown).

The synthesis of MF-6P, a previously uncharacterized disaccharide, was maximal at pH 8.0 (data not shown) and depended on the presence of Mg^{2+} or Mn^{2+} (Fig. 3*B*), with apparent K_m values of 1.5 ± 0.7 mM and 2.3 ± 1.0 mM for GDP-Man and Fru-6P, respectively (data not shown).

Taking into account the possibility that MF-6P may be the intermediate in a pathway similar to that of Suc biosynthesis and that Suc-6P and MF-6P share a similar structure, we investigated whether His_6::At-PHD was the phosphatase involved in MF-6P dephosphorylation in *A. tumefaciens*. Thus, we assayed His_6::At-PHD activity in the presence of His_6::At-GTD reaction products. Our results demonstrated the hydrolysis of MF-6P to MF and P_i (Fig. 3*C*), a reaction that also is inhibited by known phosphatase effectors (fluoride, molybdate, and orthovanadate) (data not shown). Although the recombinant At-PHD hydrolyzed Suc-6P (Fig. 3*D*), this disaccharide would not be the physiological substrate of the enzyme because Suc could not be detected in *A. tumefaciens* cells (data not shown).

The occurrence of enzyme activities that synthesized MF was confirmed in protein extracts from *A. tumefaciens* C58 cells. An MT and a phosphohydrolase activity, which produce MF-6P and MF, respectively, were separated through a DEAE-Sephacel chromatography (Fig. 4). Comparison of the biochemical and immunological properties of those enzymes with the recombinant proteins, as well as the characterization of the reaction products, indicated that the *A. tumefaciens* enzymes correspond to the At-GTD and At-PHD proteins (data not shown). Therefore, they were renamed as mannosylfructose-phosphate synthase and mannosylfructose-phosphate phosphatase, and their encoding genes as *mfpsA* and

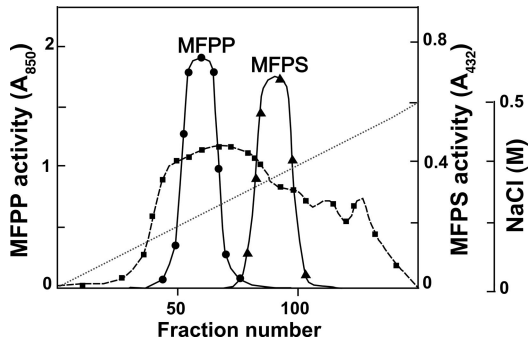

Fig. 4. Presence of MFPS and MFPP in *A. tumefaciens* cells. Protein extracts from cells grown in LB medium (containing 0.17 M NaCl) were chromatographed onto a DEAE-Sephacel column, and MFPS (triangles) and MFPP (circles) activity and proteins (squares) were determined in the collected fractions. The broken line represents the NaCl gradient.

mfppA, respectively. MF biosynthesis is proposed as a two-step pathway involving an intermediate disaccharide phosphate (Fig. 1).

MFPS and MFPP Expression. MF structure is coincidental with mannosucrose, the compatible solute reported in the salt-tolerant *A. tumefaciens* biotype I, which includes the C58 strain (6). When MFPS and MFPP expression was immunoanalyzed, both polypeptides were detected after 2 h of salt addition (Fig. 5*A*, lane 2), reaching a maximum after 5 and 6 h, respectively. The MF cell content was 7.6 ± 1.4 nmol/mg of fresh weight 24 h after the onset of the salt treatment. MF accumulation reversed when cells were transferred to a basal medium; after 2 h, the MF content returned to the level before the imposed stress. A similar reversion pattern was obtained when we immunoanalyzed MFPS and MFPP polypeptide levels (Fig. 5*A*, lanes 8 and 9). These results confirm the osmolyte role of MF, similar to what was reported for Suc in *Anabaena* sp. PCC 7120 (7).

The genomic organization of *mfpsA* and *mfppA* with four nucleotides overlapping (Fig. 2*A*) and the presence of a ribosome binding site sequence that is 13 bp upstream from *mfppA* but absent upstream from *mfpsA* predict an operon structure (8–11). Therefore, to analyze *mfpsA* and *mfppA* expression at the transcriptional level, we conducted Northern blot analyses using two different DNA probes (Fig. 2*A*) that showed coincidental signals of ≈2,100 bp (Fig. 6*A*). Thus, the occurrence of a unique bicistronic messenger was demonstrated. However, it appears that long transcripts were synthesized initially and that, subsequently, these were degraded into smaller products, as indicated by the presence of smears in the blots. Induction of the MF operon expression by salt was maximal at 3 h after NaCl addition (Fig. 6*B*).

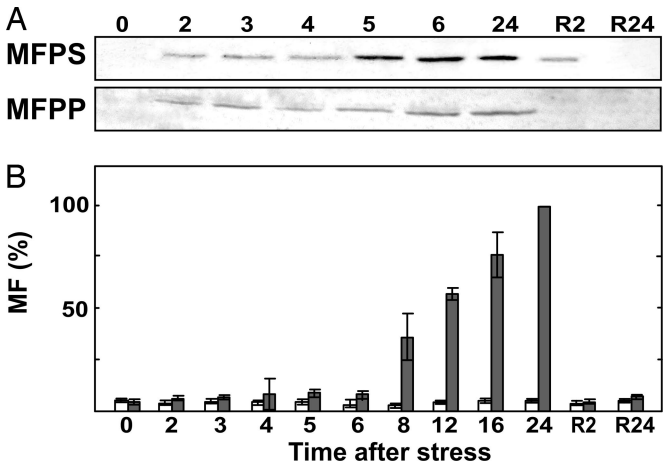

Fig. 5. Reversible effect of NaCl on MFPS and MFPP expression. (*A*) Western blot analysis. (*B*) MF accumulation in *A. tumefaciens*. Cells were grown in Ty medium for 24 h and then harvested (0 h) or added with 0.5 M NaCl. Samples were taken within 24 h at different times after salt addition. For reversion analysis, 24-h salt-stressed cells were transferred to Ty-basal medium for 2 h (R2) or 24 h (R24). Gray bars, MF accumulation in stressed cells; open bars, MF accumulation in cells kept in Ty medium. 100% corresponds to 7.6 ± 1.4 nmol/mg of fresh weight. Values are the mean ± SD; $n = 3$.

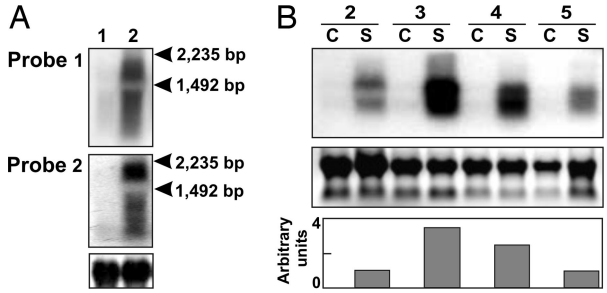

Fig. 6. Analysis of the MF operon (*mfpsA-mfppA*) expression by Northern blot. (*A*) Total RNA was prepared from control cells grown in Ty-medium (lane 1) or from 3-h-treated cells with 0.5 M NaCl (lane 2). Membranes were hybridized with probe 1 and probe 2 (see Fig. 2*A*). RNA size markers (1,492 and 2,235 bp) are indicated with arrowheads. For loading control, RNA was stained with ethidium bromide (*Bottom*). (*B*) Total RNA was purified from 0.5 M NaCl-treated cells (S) or from Ty medium-grown cells (C, control) harvested at 2, 3, 4, and 5 h of treatment. Membranes were hybridized with probe 1. Also shown are loading RNA control (*Middle*) and densitometry analysis (*Bottom*).

Phylogenetic Analysis of *A. tumefaciens* MFPS. Through BLAST searches, we retrieved MFPS homologs and generated neighbor-joining dendrograms (Fig. 7). *A. tumefaciens* MFPS together with a putative GT from *Stappia aggregata* form a separate cluster (bacterium MTs group II) that branches closer to cyanobacterial SPSs than to bacterium MTs of group I. Similar tree topologies were observed by maximum parsimony and likelihood analysis (data not shown).

Discussion

The presence of homologs to genes encoding Suc biosynthesis enzymes in genomes of heterotrophic microorganisms (2) for which there is no evidence of their ability to accumulate Suc raised a question: What is the role of their protein products? Our studies in *A. tumefaciens*, a proteobacterium that causes parasitic tumors in a wide range of plants, uncovered a metabolic pathway responsible for the biosynthesis of MF, a mannose-containing nonreducing disaccharide. This biosynthetic route is similar to those of Suc and trehalose, the main occurring nonreducing disaccharides in nature (3, 12), and it involves the sequential action of two enzymes: an MT (MFPS, GDP-Man: D-fructose-6-phosphate 2-α-D-mannosyltransferase) and a fructose-containing disaccharide phosphatase (MFPP, mannosylfructose-6^F-phosphate-phosphohydrolase) yielding MF and P_i. This two-step strategy to biosynthesize key stress response molecules (such as Suc, trehalose, and glucosylglycerol) presents the important advantage that the hydrolysis of the intermediate leads to an effectively irreversible pathway that favors the accumulation of the product (3, 12, 13).

A. tumefaciens MFPS and An-SPSs share important biochemical, immunological, and structural properties (4, 14). MFPS exhibits the motif-I signature defined for cyanobacterial and plant SPS proteins (4). Importantly, from the present evidence, that signature should not be considered as an exclusive feature of Suc metabolism glucosyltransferases. Also SPSs and MFPS sequences have been included in the GT family 4 and were recently suggested to belong

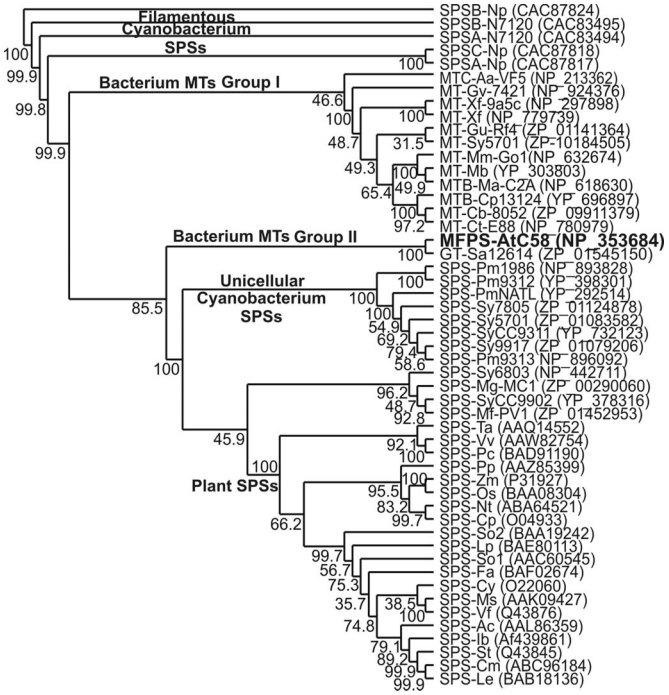

Fig. 7. Phylogenetic analysis of MFPS homologs. Unrooted trees were constructed after sequence alignments of the GTDs of MFPS homologous proteins. Numbers on nodes indicate bootstrap support (1,000 replicates). Aa, *Aquifex aeolicus* VF5; Ac, *Actinidia chinensis*; AtC58, *Agrobacterium tumefaciens* C58; Cb-8052, *Clostridium beijerincki* NCIMB 8052; Cm, *Cucumis melo*; Cp13124, *Clostridium perfringens* ATCC 13124; Cp, *Craterostigma plantagineum*; Ct-E88, *Clostridium tetani* E88; Cy, *Citrus unshiu*; Fa, *Fragaria x ananassa*; Gu-Rf4, *Geobacter uraniumreducens* Rf4; Gv-7421, *Gloeobacter violaceus* PCC 7421; Ib, *Ipomoea batatas*; Le, *Lycopersicon esculentum*; Lp, *Lolium perenne*; Mg-MC1, *Magnetococcus* sp. MC1; Ma-C2A, *Methanosarcina acetivorans* C2A; Mb, *Methanosarcina barkeri* str. Fusaro; Mf-PV1, *Mariprofundus ferrooxydans* PV-1; Mm-Go1, *Methanosarcina mazei* Go1; Ms, *Medicago sativa*; N7120, *Nostoc* (*Anabaena*) sp. PCC 7120; Np, *Nostoc punctiforme* PCC 73102; Nt, *Nicotiana tabacum*; Os, *Oryza sativa*; Pc, *Pyrus communis*; PmNATL, Pm9312, Pm1986, and Pm9313, *Prochloroccocus marinus* NATL2A, MIT9312, CCMP1986, and MIT9313, respectively; Pp, *Physcomitrella patens* subsp. Patens; Sa12614, *Stappia aggregata* IAM 12614; So, *Spinacia oleracea*; St, *Solanum tuberosum*; Sy6803, *Synechocystis* sp. PCC6803; Sy9902, Sy9917, Sy7805, Sy9311, and Sy5701, *Synechococcus* sp. CC9902, RS9917, WH7805, CC9311, and WH5701, respectively; Ta, *Triticum aestivum*; Vf, *Vicia faba*; Vv, *Vitis vinifera*; Xf and Xf-9a5c, *Xylella fastidiosa* Temecula1 and 9a5c, respectively; Zm, *Zea mays*. Accession numbers are in parentheses.

to the GT-B superfamily (15). A similar comparative analysis can be done between MFPP and An-SPP, showing related catalytic and structural properties (5). The fact that MFPP hydrolyses either MF-6P or Suc-6P was not surprising because the recent solution of the tridimensional structure of *Synechocystis* sp. PCC 6803 SPP complexed with Suc-6P, shows that the hexose 2-hydroxyl group of the Suc-6P molecule, the only feature that discriminates Suc-6P from MF-6P (Fig. 1), is not involved in the interactions with the disaccharide binding site (16).

The discovery of the MF biosynthesis pathway has initiated a new series of surprises concerning protein evolution and functional diversification. The question arises as to the origin of the biosynthesis of MF, a rare disaccharide in nature. Not only is this pathway mechanistically similar to that of Suc, but the corresponding proteins are also phylogenetically related. MFPS, which defines a previously uncharacterized MT family (Fig. 7, group II), might have shared a less remote common ancestral gene with SPSs than with other bacterium MTs (group I). We hypothesize that MF metabolism might be evolved from cyanobacterial Suc metabolism and that key changes might have occurred within the SPS sugar-donor catalytic subsite to change into an MFPS, to accommodate the additional esteric bulk of a purine nucleotide. According to that hypothesis, the specificity for the glycosyl acceptor (Fru-6P) might have been set first in the hypothetical ancestor, and the donor diversification between XDP-Glc and GDP-Man might have emerged later. Thus, the GDP-Man binding site of bacterium MTs (Fig. 7) of groups I and II might have arisen independently during the divergence of GTs.

In contrast to Suc biosynthesis proteins that are likely ubiquitous in cyanobacteria, homologs to MF biosynthesis proteins seem not to be widespread in extant bacteria, which raises a question: Were their encoding genes acquired by lateral gene transfer from cyanobacteria? The physical clustering of *mfpsA-mfppA* in an operon arrangement agrees with one of the requirements for the acquisition of a complete biosynthetic route in a single step by lateral gene transfer (17).

An interesting issue is why, in *A. tumefaciens*, the synthesis of a stress-related disaccharide takes place from a mannose nucleotide. *A. tumefaciens* is a unique plant pathogen that can genetically manipulate its host, which does not compete with the bacterium for the mannose pool. Although mannose appears to be important in the bacterium cells in response to an environmental condition (6) and as a carbohydrate source necessary for tumor establishment (18, 19), it has a toxic effect on most plants (20, 21). Thus, it can be speculated that this aspect of the plant–microbe interaction might have contributed to the acquisition of MF biosynthesis in an apparently narrow ecological niche. Although the study of the hypothetical function of *A. tumefaciens mfpsA* and *mfppA* during plant cell infection was beyond the scope of the present work, the identification of these osmotic stress genes represents a breakthrough that warrants further investigation on the plant–bacterium interaction.

To date, the MF pathway is likely to be restricted to *A. tumefaciens* and *S. aggregata* (Fig. 7 and data not shown), although homologs to genes coding for SPS and SPP can be found in about one of six bacterial genomes and also in archaeal genomes (*Acidithiobacillus ferrooxidans*, *Bacillus halodurans*, *Clostridium acetobutylicum*, *Corynebacterium glutamicum*, *Magnetococcus* sp. MC1, *Mycobacterium tuberculosis*, *Nitrosomonas europaea*, and *Methanococcus jannaschii*, among others). Whether these microbial GTD- and PHD-like ORFs are related to Suc, MF, or some other metabolite biosynthesis is still an open question. Further experimental analyses in those bacterial and archaeal species are required in order to learn the answer.

Materials and Methods

Bacterial Strains and Culture Conditions. *A. tumefaciens* C58 cells were grown in LB (22), which contains 170 mM NaCl, or Ty-basal medium (23), supplemented with rifampicin at 25 $\mu g \cdot ml^{-1}$, at 28°C with orbital shaking. Salt treatment was applied by adding 0.5 M NaCl to cultures in Ty medium at the middle of exponential phase up to 24 h of growth. Cells were harvested at different times of the treatment. Reversion experiments were carried out by filtering salt-treated cells, washing them, and transferring them to basal medium. *E. coli* strain DH5α was used as a general host strain for cloning, and BL21(DE3)pLysS was used for protein expression. Cultures were grown in LB broth or LB agar plates and supplemented with carbenicillin at 50 $\mu g \cdot ml^{-1}$ or chloramphenicol at 30 $\mu g \cdot ml^{-1}$, when required.

Cloning, Expression, and Purification. DNA sequences of ORFs *At-GTD* and *At*-PHD (named after functional characterization as *mfpsA* and *mfppA*, respectively) from the *A. tumefaciens* C58 genome were retrieved from the National Center for Biotechnology Information (NCBI), accession nos. NP_353684.1 and NP_353683.1, respectively. DNA fragments of 1,365 bp (*mfpsA*) and 747 bp (*mfppA*) were amplified by employing PCR technology and the

oligonucleotides f-mfpsA (5′-gcgtcgactggaacctttgtgctcttcggtctttttac-3′) and r-mfpsA (5′-ccaagcttaagatcggtggaaagaagacgaagcggtttcaat-3′), and f-mfppA (5′-gagtcgacttgaaaccgcttcgtcttctttt-3′) and r-mfppA (5′-ccaagctttagcgggggttcagtcc-3′), respectively. F-mfpsA and f-mfppA introduced a HindIII restriction site, and the reverse primers were designed with a XhoI restriction site (underlined above). Amplification products were ligated into the pRSET-A (Invitrogen, Carlsbad, CA) vector between the restriction sites HindIII and XhoI for *mfpsA* and *mfppA*, obtaining the recombinant plasmids pR*mfpsA* and pR*mfppA*, respectively. The identity of both constructs was confirmed by DNA sequencing. *E. coli* BL21(DE3)pLysS cells were transformed with pR*mfpsA* and pR*mfppA* to produce the recombinant proteins His_6::At-GTD (MFPS) and His_6::At-PHD (MFPP), respectively. The expression of the recombinant proteins was induced at OD_{600} 0.5–0.6 with 1 mM isopropyl-β-D-thiogalactopyranoside, and overexpression was allowed to proceed at 18°C for His_6::MFPS and 37°C for His_6::MFPP for 20 h. Cells from 1 liter of culture were pelleted by centrifugation, resuspended in 2 vol of buffer A [50 mM Hepes-NaOH (pH 7.5)/150 mM NaCl/0.5 mM phenylmethylsulphonylfluoride/7.5 mM 2-mercaptoetanol], lysed by three freezing–thawing cycles, and incubated with 2 $\mu g \cdot ml^{-1}$ DNase-RNase for 30 min at 4°C. Cell debris was removed by centrifugation, and the supernatant was incubated with 1 ml of immobilized Co^{2+} affinity chromatography resin (Talon; Clontech, Mountain View, CA) at 4°C for 1 h. After the unbound fraction was discarded, the resin was resuspended in 3 ml of buffer A, loaded onto a column, and washed with 3 ml of buffer A and 5 mM imidazole. Recombinant proteins were eluted from the column with a stepwise imidazole pH 7.0 gradient (50, 100, and 150 mM). Fractions containing the recombinant proteins were pooled and concentrated in an Amicon (Newtown, PA) ultrafiltration cell. Purified enzymes were stored at −20°C.

Purification of *A. tumefaciens* Enzymes. *A. tumefaciens* C58 cells (≈8 g of fresh weight) grown in LB medium were harvested at late exponential phase, resuspended, and disrupted in buffer containing 20 mM Hepes-NaOH (pH 6.5), 1 mM EDTA, 10 mM $MgCl_2$, 20% glycerol (vol/vol), and 5 mM 2-mercaptoetanol. The 20,000 × *g* supernatant, referred to as crude extract, was loaded onto a DEAE-Sephacel (Amersham Biosciences, Piscataway, NJ) column and bound proteins were eluted with a linear NaCl gradient from 0 to 0.5 M in equilibration buffer. Fractions with MFPS or MFPP activity were pooled and concentrated by using an Amicon ultrafiltration cell. Proteins were quantified according to Bradford (24).

Enzyme Assays. MFPS production of MF was measured by the thiobarbituric acid (TBA) method as described in ref. 14. MFPS production of GDP was determined after phosphoenolpyruvate-dependent pyruvate kinase phosphorylation of GDP and coupling of pyruvate to 2,4-dinitrophenylhydrazine (25). The incubation mixture contained 3 mM GDP-Man, 10 mM fructose-6-phosphate (Fru-6P), 100 mM Hepes-NaOH (pH 8.0), 20 mM $MnCl_2$, and an aliquot of the protein fraction. Sugar dinucleotide-phosphate specificity was measured in the presence of 10 mM XDP-glucose (X = A, U, or G), or 3 mM UDP-Man or ADP-Man, which were provided by M. Dankert and L. Ielpi (Fundación Instituto Leloir, Buenos Aires, Argentina). MFPP activity was determined by the Chifflet's method as described in ref. 26. The incubation mixture contained 3 mM GDP-Man, 10 mM Fru-6P, 100 mM Hepes-NaOH (pH 7.0), 20 mM $MgCl_2$, and an aliquot of the protein fraction.

Western Blot Analysis. An aliquot of *A. tumefaciens* C58 cell suspension (1 ml) was centrifuged for 1 min at 4°C, and the pellet was suspended in Laemmli buffer (27). Proteins were resolved on 10% (for MFPS) or 15% (for MFPP) denaturing polyacrylamide gels (SDS/PAGE). After separation, proteins were electroblotted onto nitrocellulose membranes (HyBond C; Amersham Biosciences) (described in ref. 28), which were blocked for 18 h at 4°C in a solution containing 5% of nonfat milk in Tris-buffered saline-Tween (TBS-T) [20 mM Tris·HCl (pH 7.2)/0.3 M NaCl with 0.1% Tween-20]. Membranes were incubated overnight at 4°C in 5% nonfat milk containing the appropriate rabbit polyclonal antibodies, raised against An-SPS-A or An-SPP (anti-An-SPS-A or anti-An-SPP, respectively). After washing with TBS-T, immunoreactive proteins were detected by using alkaline phosphatase-conjugated secondary antibodies. The blot was developed with nitroblue tetrazolium and 5-bromo-4-chloro-3-indolyl phosphate substrate (Sigma–Aldrich, St. Louis, MO).

Northern Blot Assays. All procedures were as described by Sambrook and Russell (22). Total RNA was isolated from *A. tumefaciens* C58 cells by the TRIzol procedure (GIBCO-BRL/Invitrogen). Up to 30 μg of total RNA was used for each individual condition. RNA was separated in a 1.2% agarose-formaldehyde denaturing gel and immobilized in positively charged nylon membranes (0.45 μm; Nytran; Schleicher & Schuell, Keene, NH), by alkaline passive transference. Two different oligonucleotide probes were designed: probe 1 of 1,074 bp (from nucleotide 869 of *mfpsA* to nucleotide 581 of *mfppA*) and probe 2 of 747 bp (the whole sequence of *mfppA*). Probes were labeled with [α-^{32}P]dCTP by the random primer extension system (NEN Life Science Products, Boston, MA). Prehybridization and hybridization of the membranes were carried out at 65°C in a mixture containing 0.5 M $NaHPO_4$ (pH 7.2), 1% bovine seroalbumin, and 7% SDS. After 18 h of hybridization, membranes were rinsed once for 5 min at 65°C in 1× SSC and 0.1% SDS, and three times for 10 min at 65°C in 0.5× SSC and 0.1% SDS. Membranes were exposed to autoradiography films (Kodak RMX, Rochester, NY) at −80°C and then revealed and fixed with Kodak products. The densitometry analysis of the signals was carried out with the program TotalLab (Fotodyne, Hartland, WI).

Sequence and Phylogenetic Analysis. Sequences were obtained from the nonredundant protein database of the National Center for Biotechnology Information by BLAST searches with An-SPSs amino-acidic sequences as query. Sequence alignments of the GTDs were generated with the ClustalX software (version 1.8). Dendrograms were compiled by using the JTT model (29) and the neighbor-joining algorithm (30) of the PHYLIP 3.66 package (31). The statistical significance of the tree topology was evaluated by bootstrap analysis (1,000 independent trials) (32). Trees were drawn with TREEVIEW (33).

We thank C. Fernández for technical assistance; Horacio Pontis, Eduardo Blumwald, and Leonardo Curatti for helpful comments on the manuscript; and Angeles Zorreguieta (Fundación Instituto Leloir, Buenos Aires, Argentina), Marcelo Dankert, and Luis Ielpi for kindly providing the *A. tumefaciens* strain and invaluable reagents. This work was supported by the Agencia Nacional de Promocion Científica y Tecnológica (PICT 2004), the Consejo Nacional de Investigaciones Científicas y Tecnológicas (PIP 6105), the Universidad Nacional de Mar del Plata, and the Fundación para Investigaciones Biológicas Aplicadas. This study is part of the Ph.D. thesis of L.L.T.

1. Bourne Y, Henrissat B (2001) *Curr Opin Struct Biol* 11:593–600.
2. Salerno GL, Curatti L (2003) *Trends Plant Sci* 8:63–69.
3. Winter H, Huber SC (2000) *Crit Rev Plant Sci* 19:31–67.
4. Cumino A, Curatti L, Giarrocco L, Salerno GL (2002) *FEBS Lett* 517:19–23.
5. Cumino A, Ekeroth C, Salerno GL (2001) *Planta* 214:250–256.
6. Smith LT, Smith GM, Madkour MA (1990) *J Bacteriol* 172:6849–6855.
7. Salerno GL, Porchia AC, Vargas WA, Abdian PL (2004) *Plant Sci* 167:1003–1008.
8. Salgado H, Moreno-Hagelsieb G, Smith TF, Collado-Vides J (2000) *Proc Natl Acad Sci USA* 97:6652–6657.
9. Deakin WJ, Furniss CS, Parker VE, Shaw CH (1997) *Gene* 189:135–137.
10. Liang Y, Aoyama T, Oka A (1998) *DNA Res* 5:87–93.
11. Ma J, Campbell A, Karlin S (2002) *J Bacteriol* 184:5733–5745.

12. Goddijn OJ, van Dun K (1999) *Trends Plant Sci* 4:315–319.
13. Marin K, Zuther E, Kerstan T, Kunert A, Hagemann M (1998) *J Bacteriol* 180:4843–4849.
14. Porchia AC, Salerno GL (1996) *Proc Natl Acad Sci USA* 93:13600–13604.
15. Kikuchi N, Narimatsu H (2006) *Biochim Biophys Acta* 1760:578–583.
16. Fieulaine S, Lunn JE, Borel F, Ferrer JL (2005) *Plant Cell* 17:2049–2058.
17. Ochman H, Lawrence JG, Groisman EA (2000) *Nature* 405:299–304.
18. Wächter R, Langhans M, Aloni R, Götz S, Weilmünster A, Koops A, Temguia L, Mistrik I, Pavlovkin J, Rascher U, *et. al.* (2003) *Plant Physiol* 133:1024–1037.
19. LaPointe G, Nautiyal CS, Chilton WS, Farrand SK, Dion P (1992) *J Bacteriol* 174:2631–2639.
20. Privalle LS (2002) *Ann NY Acad Sci* 964:129–138.
21. Stein JC, Hansen G (1999) *Plant Physiol* 121:71–80.
22. Sambrook J, Russell DW (2001) *Molecular Cloning, A Laboratory Manual* (Cold Spring Harbor Lab Press, Cold Spring Harbor, NY), 3rd Ed.
23. Beringer JE (1974) *J Gen Microbiol* 84:188–198.
24. Bradford MM (1976) *Anal Biochem* 72:248–254.
25. Cabib E, Leloir LF (1954) *J Biol Chem* 206:779–790.
26. Echeverria E, Salerno G (1994) *Plant Sci* 96:15–19.
27. Laemmli UK (1970) *Nature* 227:680–685.
28. Renahart J, Sandoval Y (1984) *Methods Enzymol* 104:455–460.
29. Jones DT, Taylor WR, Thornton JM (1992) *Comput Appl Biosci* 8:275–282.
30. Saitou N, Nei M (1987) *Mol Biol Evol* 4:406–425.
31. Felsenstein J (1997) *Syst Biol* 46:101–111.
32. Felsenstein J (1985) *Evolution (Lawrence, Kans)* 39:783–791.
33. Page RD (1996) *Comput Appl Biosci* 12:357–358.